Journal of Thermal Analysis and Calorimetry
https://doi.org/10.1007/s10973-018-7133-y

Thermal, spectral and biological investigation of new nickel complexes with imidazole derivatives

Ioana Dorina Vlaicu[1] · **Rodica Olar**[2] · **Gina Vasile Scăeţeanu**[3] · **Luigi Silvestro**[4] · **Martin Maurer**[4] ·
Nicolae Stănică[5] · **Mihaela Badea**[2]

Received: 22 November 2017 / Accepted: 24 February 2018

Abstract

Four new Ni(II) complexes with acrylate and imidazole (Him) or imidazole derivatives [2-methylimidazole(2-MeIm)/5-methylimidazole(5-MeIm)/2-ethylimidazole(2-EtIm)] as ligands were prepared and characterized. All coordination compounds were characterized by elemental analysis, infrared (FTIR) and ultraviolet-visible-near-infrared (UV-Vis-NIR) spectroscopy, mass spectroscopy, magnetic moments measurements and thermal analysis (TG). The resulted complexes were formulated as follows: $[Ni(HIm)_2(acr)_2]$ (**1**), $[Ni(2\text{-}MeIm)_2(acr)_2(H_2O)]\cdot H_2O$ (**2**), $[Ni(5\text{-}MeIm)_2(acr)_2]\cdot H_2O\cdot$ (**3**), $[Ni(2\text{-}EtIm)_2(acr)_2(H_2O)]\cdot H_2O$ (**4**). On the basis of magnetic moments measurements and on UV–Vis–NIR spectra, for all Ni(II) complexes was proposed an octahedral stereochemistry. Acrylate ions act as bidentate in complexes (**1**) and (**3**); meanwhile, in (**2**) and (**4**) they behave as bidentate and unidentate. Antimicrobial activity of complexes was investigated on ATCC reference and clinical microbial strains. The MIC (minimum inhibitory concentration) values revealed moderate antimicrobial activity of complex (**1**) against *Enterococcus faecium* and of complex (**2**) against *Pseudomonas aeruginosa* and *Bacillus subtilis*.

Keywords Imidazole derivative · Nickel complex · Thermal analysis · Acrylate

Introduction

The coordination chemistry of carboxylates and azoles is very interesting and lately has gained interest having in view the versatility of carboxylate anions, and due to potential biological activities of resulted complexes, the more so as the azole ligands are reported for antimicrobial, antiviral, antidiabetic, anticancer activities [1]. Complexes with azole-type ligands are in our interest for several years, and their biological potential has been evidenced in some papers [2–7].

Imidazole core, found in many bioactive heterocyclic compounds, has the potential to generate new species used for treatment of cancer, metabolic disorders and infectious diseases [8]. Beside organic compounds based on imidazole nucleus with proven pharmacological activities [8], there are reported imidazole-containing metal complexes with significant biological properties. So far, bis(acetato)tetrakis(imidazole) copper(II) complex presents anticonvulsant activity against strychnine [9] and hypoglycemic effect [10]. The hypoglycemic effect, but less pronounced, has been manifested also by bis(acetato)bis(μ-acetato)tetrakis(*N*-methylimidazole) copper(II) hexaaquo and bis(acetato)bis(1,2-dimethylimidazole)copper(II) [10]. Other complexes with general formula $[Cu(dien)(B)(NO_3)](NO_3)$ (dien = diethylenetriamine,

---

✉ Mihaela Badea
e_m_badea@yahoo.com

[1] National Institute of Materials Physics, Atomistilor Str. 405A, POB MG-7, 077125 Măgurele, Ilfov, Romania

[2] Department of Inorganic Chemistry, Faculty of Chemistry, University of Bucharest, 90-92 Panduri Str., 050663 Bucharest, Romania

[3] Department of Soil Sciences, University of Agronomical Sciences and Veterinary Medicine, 59 Mărăşti Str., 011464 Bucharest, Romania

[4] 3S-Pharmacological Consultation and Research GmbH, 1 Koenigsbergerstrasse, 27243 Harpstedt, Germany

[5] "Ilie Murgulescu" Physical Chemistry Institute, Romanian Academy, 202 Splaiul Independentei, 77208 Bucharest, Romania

B = imidazole/2-ethylimidazole) have presented activity against colon cancer cells (HT-29) [11]. Also, complexes of copper(II) with carboxylate and imidazole ligands have been studied as models for copper proteins that contain both functionalities in the side chain [12, 13].

Complexes of the type $[Cd(valp)_2(imidazole)_2]$, $[Co(valp)_2(imidazole)_2]$ (valp = valproate) exhibit cytotoxic specificity, a significant cancer cell inhibitory rate against tumor cell lines (HeLa, Hep-G2, A2780, LS-174, B16, MS1, MRC-5), and present antibacterial activity against Gram-positive and Gram-negative bacteria [14].

In addition to those mentioned above, there are reported two categories of complexes that present imidazole core and carboxylates: (**i**) mixed ligand complexes based on imidazole/imidazole derivative and various carboxylates and (**ii**) complexes with ligands that present grafted both imidazole and carboxylate groups.

Accordingly, complexes $Zn(im)_2(L2)_2$ (im = imidazole, L2 = 3-(4-methoxyphenyl)acrylate), $Zn(im)_2(L3)_2$ (L3 = methylenedioxy)benzoate) and $[Cd(im)_2(L3)_2]_2 \cdot 4H_2O$ contain imidazole coordinated in a monodentate fashion with their neutral nitrogen groups; meanwhile, carboxylate acts as monodentate, chelating bidentate and bridging bidentate. In all complexes, beside classical hydrogen bonds, there appear intra- and intermolecular weak interactions C–H···O, $CH_2 \cdots O$, $CH_3 \cdots O$, C–H···π, $CH_3 \cdots \pi$, O–H···π and π–π which are responsible for high-dimensional ordered supramolecular network [15].

The versatility of carboxylate was allowed in the case of some systems formed from copper(II) acrylate/methacrylate and imidazole to obtain more than one product from the same synthesis [16]. Hence, complexes bis(acrylate)-bis(imidazole) copper(II) (purple) and binuclear tetrakis(μ_2-acrylate-O,O′)-bis(imidazole)-dicopper(II) (green) resulted from the system $Cu_2(acrylate)_4(H_2O)_2$ and imidazole; meanwhile, bis(methacrylate)-bis(imidazole)-copper(II) (purple) and tetrakis(μ_2-α-methacrylate-O,O′)-bis(imidazole)-dicopper(II) (green) were obtained after reaction between $Cu_2(methacrylate)_4(H_2O)_2$ and imidazole. Moreover, for the reported complexes the interconversion of the two corresponding complexes with different structures in methanol solution was observed, while this behavior does not occur in anhydrous methanol. A copper(II) dimer, $[Cu_2(Ac)_4(EtImH)_2]$ (Ac = acetate, EtImH = 2-ethylimidazole), with relatively high thermal stability (close to 175 °C) probably because the presence of strong intermolecular hydrogen bridge has been reported [17]. Other studies [18] present the synthesis and structural characterization of trinuclear copper(II) complexes of the type $Cu_3(acrylate)_5(OH)(imH)_3$ and $Cu_3(methacrylate)_5(OH)(imH)_3$ (imH = imidazole) with one copper ion in a distorted trigonal bipyramidal configuration and two copper ions in a distorted square planar configuration.

Some researches present the synthesis and characterization of complexes with ligands that bear both carboxylate and imidazole groups to build coordination polymers. Consequently, there are reported [19] three coordination polymers of Cu(II), Co(II) and Ni(II) with 2-(3-methoxyphenyl)-1*H*-imidazole-4,5-dicarboxylic acid that present 1D column-like structure and display a 3D supramolecular network generated by $\pi \cdots \pi$ stacking or hydrogen bond interactions. Interesting structures and properties were obtained also in the case of employment in coordination compounds of 1*H*-imidazole-4,5-dicarboxylic acid, 1*H*-imidazole-2-carboxylic acid [20], 2-propyl-4,5-imidazoledicarboxylate [21], 2-(4-carboxyphenyl)-1*H*-imidazole-4,5-dicarboxylic acid and 2-(2-carboxyphenyl)-1*H*-imidazole-4,5-dicarboxylic acid [22].

In our ongoing interest to synthesize and characterize mixed complexes with unsaturated carboxylates and azole-type ligands [3–5], we report herein the synthesis and characterization of four new Ni(II) complexes with acrylate (acr) and imidazole (Him) or imidazole derivatives (2-methylimidazole(2-MeIm)/5-methylimidazole(5-MeIm)/2-ethylimidazole(2-EtIm)) as ligands, as follows:

$[Ni(HIm)_2(acr)_2]$ (**1**)
$[Ni(2\text{-}MeIm)_2(acr)_2(H_2O)] \cdot H_2O$ (**2**)
$[Ni(5\text{-}MeIm)_2(acr)_2] \cdot H_2O$ (**3**)
$[Ni(2\text{-}EtIm)_2(acr)_2(H_2O)] \cdot H_2O$ (**4**)

The complexes were characterized by elemental analysis, infrared (FTIR) and near-infrared–ultraviolet–visible (NIR–UV–Vis) spectroscopy, mass spectroscopy, magnetic moments measurements and thermal analysis (TG).

Experimental

Materials and methods

All chemicals were purchased from Acros Organics $[NiCO_3 \cdot 2Ni(OH)_2 \cdot 6H_2O]$, Sigma-Aldrich (imidazole and imidazole derivatives) and Merck Schuchardt OHG (acrylic acid), were of reagent grade and were used without further purification.

The chemical analyses (C, H, N) were performed on a PerkinElmer PE 2400 analyzer. Nickel content was established using a Shimadzu AA 6300 spectrometer.

IR spectra, in KBr pellets, were recorded with a Bruker Tensor 37 spectrometer in the range 400–4000 cm^{-1}.

UV–Vis–NIR spectra were recorded in the range 200–1500 nm, on a Jasco V 670 spectrophotometer, by diffuse reflectance technique, with Spectralon as standard.

Magnetic measurements were recorded at room temperature, on a Lake Shore's fully integrated vibrating sample magnetometer (VSM) system 7404 and calibrated with a Ni sphere. The molar magnetic susceptibilities were calculated and corrected for the atomic diamagnetism.

Mass spectrometry measurements were taken using a Thermo Finnigan MAT-900S mass spectrometer with FAB (Cs-gun, Thermo Finnigan) ionization source operating in positive ion mode. Samples were dissolved in a matrix of nitrobenzyl alcohol containing 1% of hydrochloric acid at 30%. Molecular ion scanning range (*m*/*z*) was 60–1450.

The heating curves (TG and DTA) were recorded using a Labsys 1200 SETARAM instrument, over the temperature range of 30–900 °C using a heating rate of 10 °C min^{-1}. The measurements were taken in synthetic air atmosphere (flow rate 16.66 $\text{cm}^3\ \text{min}^{-1}$), by using alumina crucibles.

The X-ray powder diffraction patterns were collected on a DRON-3 diffractometer with a nickel filtered Cu K_α radiation ($\lambda = 1.5418$ Å) in 2θ range of 5–70°, a step width of 0.05° and an acquisition time of 2 s per step.

The antimicrobial activities of the complexes were determined against ATCC reference and clinical microbial strains, i.e., Gram-positive (*Bacillus subtilis* ATCC 6683, *Enterococcus faecium* E5), Gram-negative (*Klebsiella pneumoniae* IC 13420, *Escherichia coli* ATCC 25922, *Pseudomonas aeruginosa* ATCC 27857) and fungus *Candida albicans* 1760.

The qualitative screening was performed by an adapted disk diffusion method, while the quantitative assay of the antimicrobial activity was performed by the liquid-medium microdilution method as previously reported [5].

Synthesis of complexes

All the complexes were obtained following the general procedure: A suspension of $NiCO_3 \cdot 2Ni(OH)_2$ (3 mmol) in methanol (50 cm^3) and acrylic acid (18 mmol) was stirred at 50 °C for 2 days. The solution of nickel acrylate obtained after filtration was then mixed with imidazole/imidazole derivative (15 mmol), stirred 2 h at room temperature and let to slow evaporation for a few days when the complex precipitate. The sparingly soluble product was filtered off, washed several times with methanol and air-dried.

$[Ni(HIm)_2(acr)_2]$. Analysis, found: Ni, 17,12; C, 42,84; H, 4,32; N, 16,42%; calculated for $NiC_{12}H_{14}N_4O_4$ (F.W. = 336,96): Ni, 17,42; C, 42,77; H, 4,19; N, 16,63%.

$[Ni(2\text{-}MeIm)_2(acr)_2(H_2O)] \cdot H_2O$. Analysis, found: Ni, 14,52; C, 41,85; H, 5,71; N, 13,78%; calculated for $NiC_{14}H_{22}N_4O_6$ (F.W. = 401,04): Ni, 14,64; C, 41,93; H, 5,53; N, 13,97%.

Exp.(%)/calc.(%): Ni, 14,52/14,64; C, 41,85/41,93; H, 5,71/5,53; N, 13,78/13,97.

$[Ni(5\text{-}MeIm)_2(acr)_2] \cdot H_2O$. Analysis, found: Ni, 15,44; C, 43,85; H, 5,37; N, 14,78%; calculated for $NiC_{14}H_{20}N_4O_5$ (F.W. = 383,03): Ni, 15,32; C, 43,90; H, 5,26; N, 14,63%.

$[Ni(2\text{-}EtIm)_2(acr)_2(H_2O)] \cdot H_2O$; Analysis, found: Ni, 13,61; C, 44,90; H, 6,16; N, 13,13%; calculated for $NiC_{16}H_{26}N_4O_6$ (F.W. = 429,09): Ni, 13,67; C, 44,78; H, 6,10; N, 13,06%.

The obtained complexes are soluble in water, methanol, ethanol, dimethylformamide and dimethylsulfoxide.

Results and discussion

As an extension of previously reported studies [3–5] and considering our interest regarding complexes with unsaturated carboxylates and azole-type ligands, new Ni(II) complexes with acrylate (acr) and imidazole (Him) or imidazole derivatives (2-methylimidazole(2-MeIm)/5-methylimidazole(5-MeIm)/2-ethylimidazole(2-EtIm)) as ligands were synthesized and characterized and formulated as $[Ni(HIm)_2(acr)_2]$ (**1**), $[Ni(2\text{-}MeIm)_2(acr)_2(H_2O)] \cdot H_2O$ (**2**), $[Ni(5\text{-}MeIm)_2(acr)_2] \cdot H_2O$ (**3**), $[Ni(2\text{-}EtIm)_2(acr)_2(H_2O)] \cdot H_2O$ (**4**). The characterization and biological activity of above-mentioned complexes are presented in the following sections.

Infrared spectra

In order to establish the nature of donor atoms and coordination mode of ligands, the infrared spectra of the ligands and the metal complexes have been recorded. The main absorption bands of imidazole, 2-methylimidazole, 5-methylimidazole and 2-ethylimidazole as well as for their complexes are listed in Table 1.

All complexes spectra display the characteristic vibration bands of imidazole-type ligands [23, 24]. The fundamental stretching vibration mode characteristic of the secondary amine group, ν(NH), occurs around 3140 cm^{-1} in complexes spectra, similar to spectra of uncoordinated ligands. In the complexes spectra, the strong band around 1640 cm^{-1} is assigned to the vibration mode ν(C=N). This band is shifted to lower wavenumbers by 35–40 cm^{-1} compared to the spectra of free imidazole/imidazole derivatives. These aspects indicate the coordination of imidazole/imidazole derivatives to metal by pyridine-type nitrogen atom.

The two band characteristics of the vibration modes ν_{as}(COO) and ν_s(COO) of the acrylate anion appear in the 1530–1580 and 1330–1420 cm^{-1} ranges. The coordination mode of acrylate anion can be assigned by comparing to the sodium acrylate spectrum, using the values of difference $\Delta = \nu_{as}(COO) - \nu_s(COO)$ [25, 26]. Thus, a

Table 1 Characteristic absorption bands (cm^{-1}) in IR spectra of ligands and complexes

HIm	2-MeIm	5-MeIm	2-EtIm	(**1**)	(**2**)	(**3**)	(**4**)	Assignments
–	–	–	–	–	3450 w	3383 w	3445 vs	$\nu(OH_2)$
3124 m	3136 m	3136 m	3153 w	3120 w	3131 w	3145 w	3150 w	$\nu(CH)$, $\nu(NH)$
–	–	–	–	2920 w	2920 w	2926 w	2920 w	$\nu_{as}(CH_2)$
–	–	–	–	2880 w	2880 w	2877 w	2880 w	$\nu_s(CH_2)$
1669 m	1676 m	1676 m	1673 w	1629 m	1640 s	1639 m	1637 vs	$\nu(C{=}N)$
–	–	–	–	1569 vs	1573 vs	1572 vs	1577 vs	$\nu_{as}(COO)$
1541 s	1596 vs	1596 vs	–	1545 s	–	–	–	$\delta(NH)$, $\nu(CC)$, $\nu(CN)$
–	–	–	–	1520 w	1520 w	–	–	$\nu(C{=}C)$ aliph
–	–	–	–	1385 m	1427 vs 1361 s	1384 m	1424 vs 1360 m	$\nu_s(COO)$
–	–	–	–	1268 s	1272 s	1273 m	1280 m	$\delta(CH_2)$
1243 w	1206 w	1206 w	1243 w	1230 w	1192 s	–	1237 m	$\nu(CN)$, $\delta(CH)$
1146 s	1155 vs	1155 vs	1153 m	1150 w	1145 w	1195 m	1150 w	$\nu(CC)$, $\nu(CN)$, $\delta(CH)$
936 vs	942 s	942 s	956 s	950 m	937 m	961 w	960 w	$\delta(CH)$, δ(imidazole ring)
895 m	875 w	875 w	875 w	885 w	875 w	875 w	875 w	$\pi(CH)$, δ(imidazole ring)
–	–	–	–	–	831 s	–	822 w	$\rho_r(OH_2)$
756 s	756 vs	756 vs	751 vs	760 m	746 m	740 w	770 w	$\pi(CH)$
619 s	627 w	627 w	625 w	647 m	679 s	621 m	625 w	$\pi(NH)$

vs—very strong, s—strong, m—medium, w—weak (band intensity in FTIR spectra); HIm—imidazole; 2-MeIm—2-methylimidazole; 5-MeIm—5-methylimidazole; 2-EtIm—2-ethylimidazole; (**1**)—$[Ni(HIm)_2(acr)_2]$; (**2**)—$[Ni(2\text{-}MeIm)_2(acr)_2(H_2O)]\cdot H_2O$; (**3**)—$[Ni(5\text{-}MeIm)_2(acr)_2]\cdot H_2O$; (**4**)—$[Ni(2\text{-}EtIm)_2(acr)_2(H_2O)]\cdot H_2O$; ν—stretching; δ—in-plane bending; π—out-of-plane bending; ρ—rocking

difference between the vibration modes of the acrylate anion, Δ, in the range of 144–153 cm^{-1} and in the range of 212–217 vs. 203 cm^{-1} for sodium acrylate indicates both bidentate and unidentate nature for complexes $[Ni(2\text{-}MeIm)_2(acr)_2(H_2O)]\cdot H_2O$ (**2**) and $[Ni(2\text{-}EtIm)_2(acr)_2(H_2O)]\cdot H_2O$ (**4**). For complexes $[Ni(HIm)_2(acr)_2]$ (**1**) and $[Ni(5\text{-}MeIm)_2(acr)_2]\cdot H_2O$ (**3**), the difference Δ of 184 and 188 cm^{-1}, respectively, indicates the bidentate nature of this ligand.

The broadband around 3400 cm^{-1} that appears in the complex combinations (**2**)–(**4**) can be assigned to the stretching vibration $\nu(OH)$ corresponding to the water molecules, their presence being confirmed by the chemical and thermal analysis. For complexes (**2**) and (**4**), the band around 830 cm^{-1} assigned to vibration mode $\rho_r(H_2O)$ indicates that water molecules are also involved in the coordination process [27].

Magnetic and electronic spectral data

The characteristics of the metal–ligand bond and the symmetry of coordination polyhedron were established on the basis of observed transitions in the UV–Vis–NIR spectra.

All complexes exhibit UV–Vis–NIR spectra (Fig. 1), characteristic of d–d transitions for Ni(II) ion in an octahedral stereochemistry [28]. In addition, a strong ultraviolet band due to the intraligand transition appears in the 41,000–46,000 cm^{-1} range. The absorptions bands for the metal complexes together with crystal-field parameters (calculated using König's formulas [29]) are listed in Table 2.

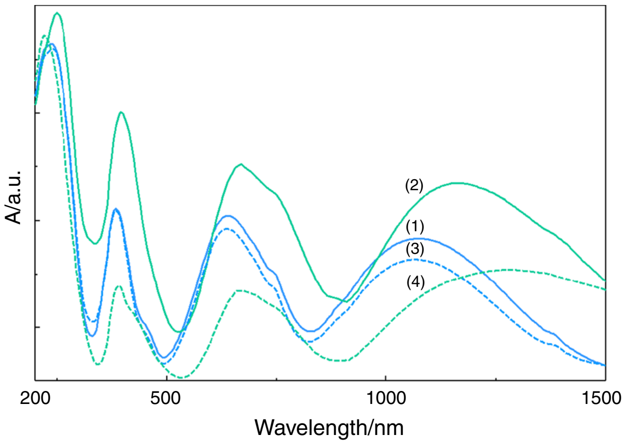

Fig. 1 UV–Vis–NIR spectra of complexes (**1**)–(**4**)

The low value of the splitting parameters is generated by the ligands' low field associated with the presence of the oxygen donor atoms. This assumption is supported by the values of the nephelauxetic parameter which corresponds

Table 2 UV–Vis–NIR absorption bands, crystal-field parameters and magnetic moments for complexes (**1**)–(**4**)

Complex	Absorption maxima/cm^{-1}	Assignments	Crystal-field parameters			μ_{ef}/B.M.
			10Dq/cm^{-1}	B/cm^{-1}	β	
[Ni(HIm)$_2$(acr)$_2$] (**1**)	41,670	$\pi \rightarrow \pi^*$	9640	845	0.81	2.98
	25,975	$^3A_{2g} \rightarrow {}^3T_{1g}$ (P)				
	22,220	$^3A_{2g} \rightarrow {}^1A_{1g}$				
	15,625	$^3A_{2g} \rightarrow {}^3T_{1g}$ (F)				
	13,515	$^3A_{2g} \rightarrow {}^1E_g$				
	9300	$^3A_{2g} \rightarrow {}^3T_{2g}$				
[Ni(2-MeIm)$_2$(acr)$_2$(H$_2$O)]·H$_2$O (**2**)	40,000	$\pi \rightarrow \pi^*$	9125	858	0.82	3.46
	25,315	$^3A_{2g} \rightarrow {}^3T_{1g}$ (P)				
	14,925	$^3A_{2g} \rightarrow {}^3T_{1g}$ (F)				
	13,515	$^3A_{2g} \rightarrow {}^1E_g$				
	8620	$^3A_{2g} \rightarrow {}^3T_{2g}$				
[Ni(5-MeIm)$_2$(acr)$_2$]·H$_2$O (**3**)	41,670	$\pi \rightarrow \pi^*$	9637	845	0.81	3.00
	25,975	$^3A_{2g} \rightarrow {}^3T_{1g}$ (P)				
	22,470	$^3A_{2g} \rightarrow {}^1A_{1g}$				
	15,625	$^3A_{2g} \rightarrow {}^3T_{1g}$ (F)				
	13,515	$^3A_{2g} \rightarrow {}^1E_g$				
	9380	$^3A_{2g} \rightarrow {}^3T_{2g}$				
[Ni(2-EtIm)$_2$(acr)$_2$(H$_2$O)]·H$_2$O (**4**)	45,455	$\pi \rightarrow \pi^*$	8990	900	0.86	3.44
	25,640	$^3A_{2g} \rightarrow {}^3T_{1g}$ (P)				
	23,810	$^3A_{2g} \rightarrow {}^1A_{1g}$				
	14,815	$^3A_{2g} \rightarrow {}^3T_{1g}$ (F)				
	13,420	$^3A_{2g} \rightarrow {}^1E_g$				
	7810	$^3A_{2g} \rightarrow {}^3T_{2g}$				

to a high degree of ionicity of metal–ligand bonds as a result of the interaction with the acrylate anion.

The values of magnetic moment lie in the 2.80–3.50 B.M. range, which is characteristic for octahedral complexes of nickel (II) [30].

Mass spectra

The mass spectra were recorded in positive ionization mode and contain peaks corresponding to pseudomolecular ion [Ni(L$_2$acr$_2$ + H]$^+$ ion at *m/z*: 337/365/365/393 for complexes (**1**)/(**2**)/(**3**)/(**4**), respectively. Also, some other fragments were evidenced: [NiL$_2$acr]$^+$ (*m/z*: 265/-/293/321), [NiLacr$_2$ + H]$^+$ (*m/z*: 269/283/-/297), [NiLacr]$^+$ (*m/z*: 197/211/211/225) as well as the protonated ligands [L + H]$^+$ (*m/z*: 69/83/83/97). Figure 2 illustrates mass spectrum of complex (**3**).

These data together with that obtained from elemental and thermal analysis confirm the complexes formulation.

Proposed coordination for nickel(II) complexes (1)–(4)

Taking into account all experimental data, the most probable coordination is presented in Fig. 3. On the basis of higher intensity of *d*–*d* transition bands which suggests a lower symmetry, for complexes (**1**)–(**3**) it was considered a *cis* position of imidazole derivatives.

Thermal behavior of complexes

The results concerning the thermal decomposition of the new complexes are presented in Table 3.

Thermal decomposition of [Ni(HIm)$_2$(acr)$_2$] (1)

According to the TG curve (Fig. 4), the complex [Ni(HIm)$_2$(acr)$_2$] (**1**) is stable up to 270 °C indicating the absence of any lattice or coordinated water/methanol molecules. The first mass loss step corresponds to oxidative degradation of both imidazole molecules. The DTG curve shape indicates this step is not a single one but an overlap

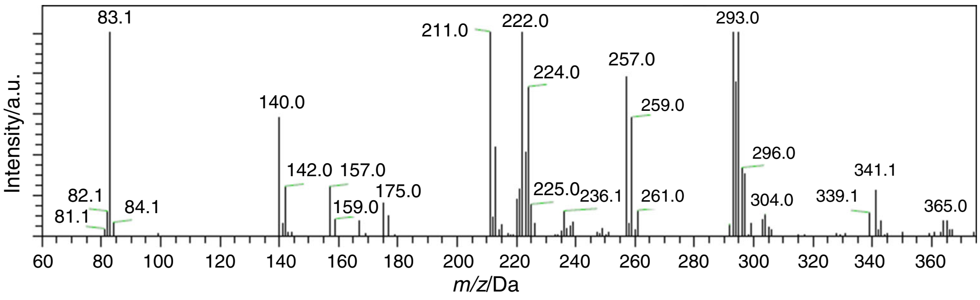

Fig. 2 Mass spectrum of complex (**3**)

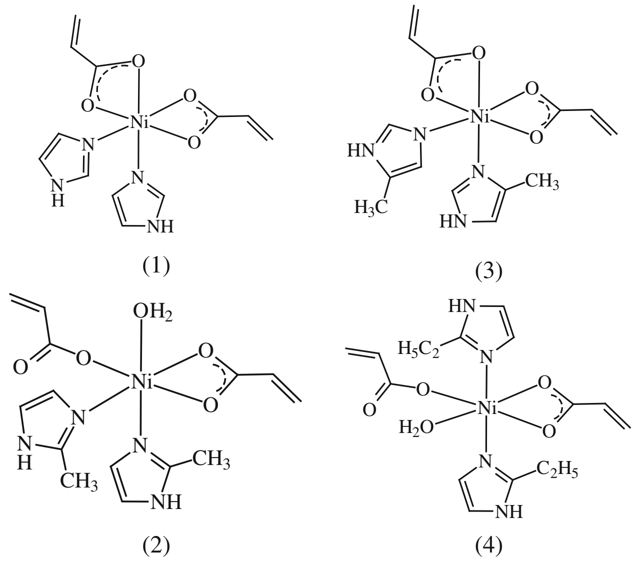

Fig. 3 Proposed coordination of complexes (**1**)–(**4**)

of at least two processes. The same information is provided by DTA curve which exhibits at least two exothermic effects. The IR spectrum of the intermediate residue isolated at 380 °C displays only the characteristic bands of acrylate ion [25]. The second exothermic decomposition step corresponds to oxidative degradation of acrylate ions, a complex process according to both DTG and DTA curves. The final residue was identified, using powder X-ray diffraction, as nickel (II) oxide.

Thermal decomposition of [Ni(2-MeIm)$_2$(acr)$_2$(H$_2$O)]·H$_2$O (2)

The thermal decomposition of title compound (Fig. 5) starts with water molecules release. Although TG curve indicates only one process, both DTG and DTA curves show successive elimination. The high temperature observed for this process suggests that apart from the fact that one molecule is coordinated, the lattice water is

Table 3 Thermal decomposition data (in air flow) for complexes (**1**)–(**4**)

Complex	Step	Thermal effect	Temp./°C	Δm_{exp}/%	Δm_{calc}/%
[Ni(HIm)$_2$(acr)$_2$] (**1**)	1.	Exothermic	270–380	40.2	40.4
	2.	Exothermic	380–490	37.4	37.4
	Residue (NiO)			22.4	22.2
[Ni(2-MeIm)$_2$(acr)$_2$(H$_2$O)]·H$_2$O (**2**)	1.	Endothermic	140–250	9.1	9.0
	2.	Miscellaneous	260–392	40.8	40.9
	3.	Exothermic	392–580	31.4	31.5
	Residue (NiO)			18.7	18.6
[Ni(5-MeIm)$_2$(acr)$_2$]·H$_2$O (**3**)	1.	Endothermic	126–160	4.9	4.7
	2.	Endothermic	250–350	21.6	21.4
	3.	Exothermic	350–460	21.2	21.4
	4.	Exothermic	460–655	32.6	33.0
	Residue (NiO)			19.7	19.5
[Ni(2-EtIm)$_2$(acr)$_2$(H$_2$O)]·H$_2$O (**4**)	1.	Endothermic	67–135	4.5	4.2
	2.	Endothermic	135–220	4.4	4.2
	3.	Exothermic	220–455	45.0	44.8
	4.	Exothermic	455–860	28.6	29.4
	Residue (NiO)			17.5	17.4

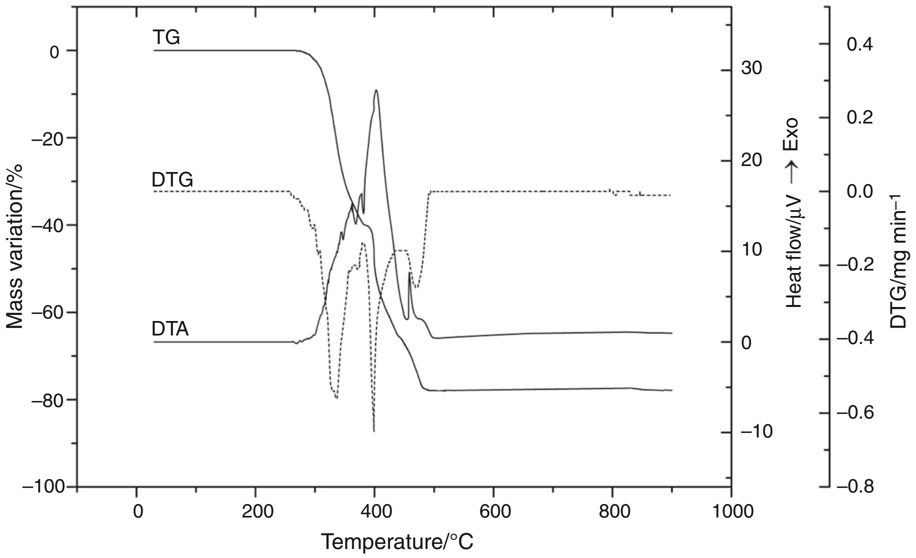

Fig. 4 Thermoanalytical curves (TG, DTG and DTA) of $[Ni(HIm)_2(acr)_2]$ in air flow at 10 °C min^{-1}

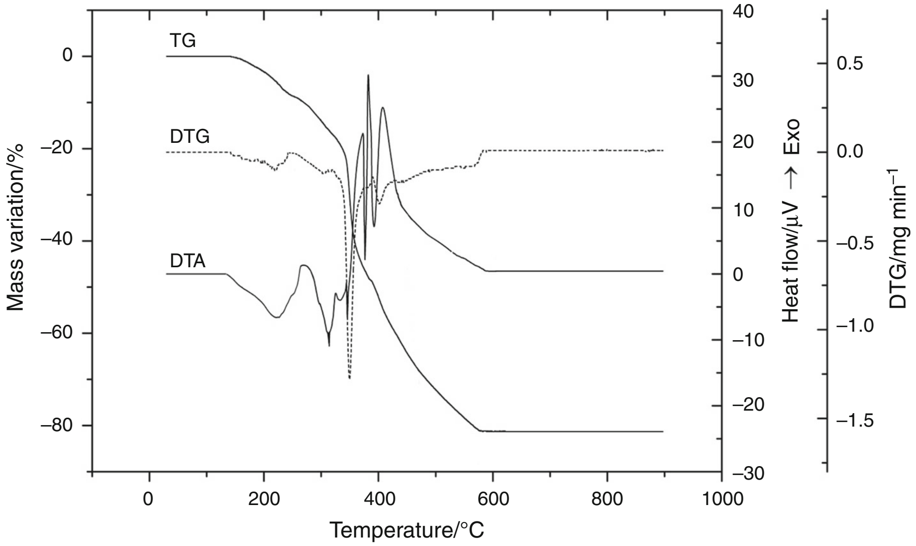

Fig. 5 Thermoanalytical curves (TG, DTG and DTA) of $[Ni(2\text{-}MeIm)_2(acr)_2(H_2O)]\cdot H_2O$ in air flow at 10 °C min^{-1}

involved in hydrogen bonds. According to the mass loss, the next step corresponds to 2-methylimidazole molecule release. The IR spectrum of intermediate isolated at 392 °C exhibits only the characteristic pattern of acrylate ion. DTA curve exhibits an endothermic effect followed by an exothermic one. In the last step, the acrylate ion oxidative degradation occurs, leading to nickel oxide as the final residue according to powder X-ray diffractogram pattern.

Thermal decomposition of $[Ni(5\text{-}MeIm)_2(acr)_2]\cdot H_2O$ (3)

The complex $[Ni(5\text{-}MeIm)_2(acr)_2]\cdot H_2O$ (**3**) decomposes in four steps (Fig. 6). First, water molecule is released in a lower-temperature range compared with the previously discussed complexes, suggesting that is not coordinated at nickel ion.

The second step which is endothermic corresponds to the loss of one molecule of imidazole derivative. IR spectrum of intermediate isolated at 350 °C (Fig. 7a) contains both 5-methylimidazole and acrylate ion characteristic bands. As temperature increases, the second molecule of 5-methylimidazole undergoes oxidative degradation. According to both DTG and DTA curves, this step is not a single one but an overlapping of two processes. The acrylate intermediate formation at 460 °C was confirmed through IR spectrum (Fig. 7b). The last step corresponds to oxidative degradation of acrylate ions, the final residue being nickel oxide.

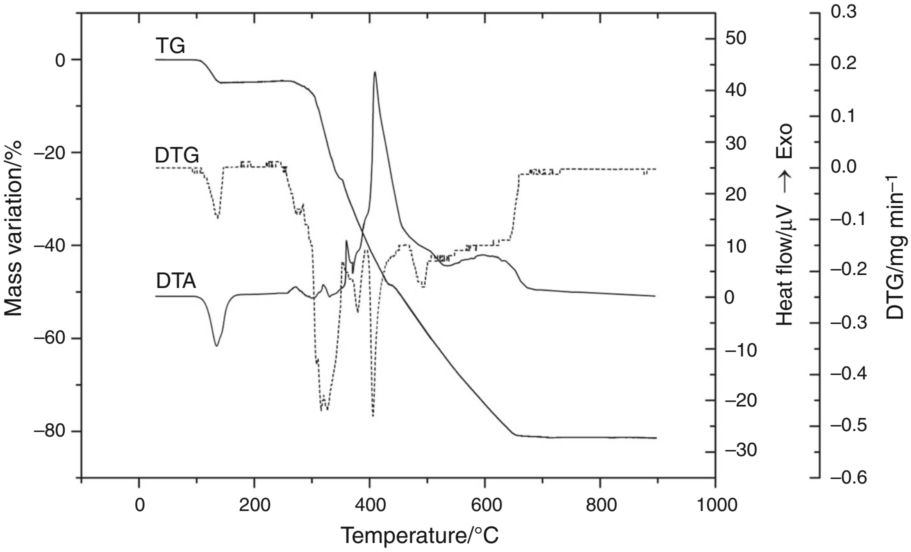

Fig. 6 Thermoanalytical curves (TG, DTG and DTA) of [Ni(5-MeIm)$_2$(acr)$_2$]·H_2O in air flow at 10 °C min^{-1}

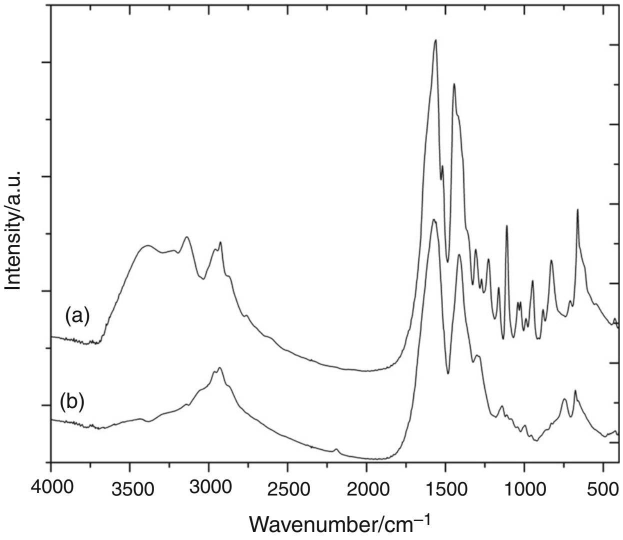

Fig. 7 IR spectra of intermediates isolated at 350 °C (**a**) and 460 °C (**b**)

Thermal decomposition of [Ni(2-EtIm)$_2$(acr)$_2$(H_2O)]·H_2O (4)

Although the thermal behavior of complex (**4**) is quite similar to the previously discussed complexes, there are some differences which are worth highlighting (Fig. 8). Thus, the different nature of water molecules is better evidenced on all thermoanalytical curves (TG, DTG and DTA) which exhibit two successive endothermic steps. This behavior was evidenced for other similar [5] or different complexes [6, 7, 31]. The imidazole derivative molecules undergo oxidative degradation in the third exothermic step as IR spectrum of intermediate indicates. The remaining nickel acrylate undergoes oxidative decomposition leading to NiO.

As a general observation, for [Ni(R-imid)$_2$(acr)$_2$] moiety there was evidenced a correlation between the molecular weight of imidazole derivative and the initial and final decomposition temperature. Thus, as the molecular weight increases, this moiety starts to decompose at lower temperatures, while the final temperature of decomposition increases.

Microbiological assay

The antimicrobial activity of complexes was investigated on ATCC reference and clinical microbial strains. Since in the first step, the qualitative screening, all compounds present diameters of inhibition zone of about 8 mm, it was proceeded to the quantitative assay. The MIC (minimum inhibitory concentration) values revealed moderate antimicrobial activity, as follows:

- complex (**1**) against *Enterococcus faecium*, (MIC 250 μg mL^{-1});
- complex (**2**) against *Pseudomonas aeruginosa* (MIC 250 μg mL^{-1}) and *Bacillus subtilis* (MIC 250 μg mL^{-1}).

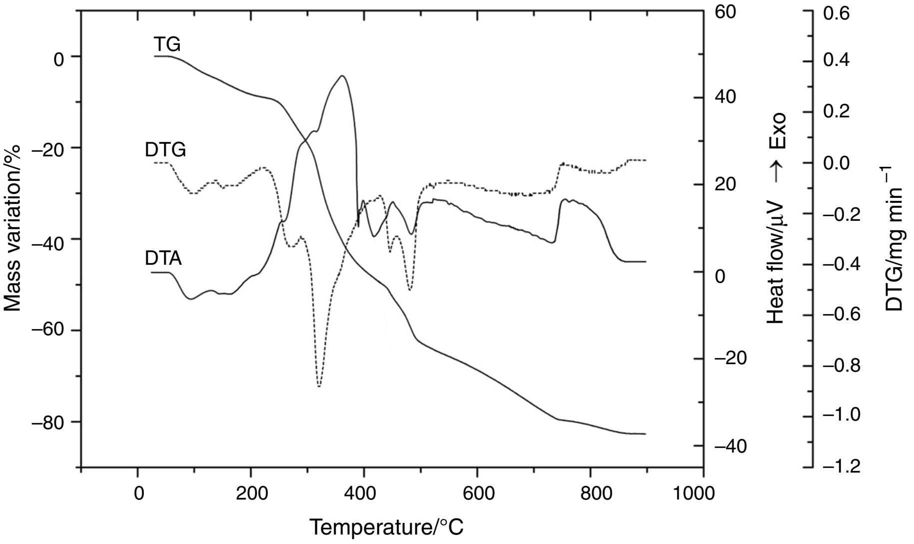

Fig. 8 Thermoanalytical curves (TG, DTG and DTA) of [Ni(2-EtIm)$_2$(acr)$_2$(H$_2$O)]·H$_2$O in air flow at 10 °C min^{-1}

Conclusions

The new complexes of Ni (II) with acrylate and imidazole (Him) or imidazole derivatives (2-methylimidazole (2-MeIm)/5-methylimidazole (5-MeIm)/2-ethylimidazole (2-EtIm)) have been synthesized and characterized. Spectral data indicate an octahedral stereochemistry for all complexes and bidentate coordination mode for acrylate in complexes (**1**) and (**3**) and both unidentate and bidentate in (**2**) and (**4**). Thermal analysis (TG, DTA) of these complexes confirms the complexes composition and allows the number and nature of the water molecule determination. A correlation between the stability of the anhydrous compounds and the molecular weights of imidazole derivatives has been established.

The MIC (minimum inhibitory concentration) values revealed moderate antimicrobial activity of complex (**1**) against *Enterococcus faecium* and of complex (**2**) against *Pseudomonas aeruginosa* and *Bacillus subtilis*.

Acknowledgements The authors thank to Mariana Carmen Chifiriuc from Faculty of Biology, University of Bucharest for the help with antimicrobial assay. I.D. Vlaicu acknowledges the financial support to the Sectorial Operational Programme Human Resources Development (SOP HRD), financed from the European Social Fund and by the Romanian Government under the contract number SOP HRD/107/1.5/S/82514. This work was partially supported by University of Bucharest.

References

1. Singh N, Pandurangan A, Rana K, Anand P, Ahamad A, Tiwari AK. Benzimidazole: a short review of their antimicrobial activities. Int Curr Pharm J. 2012;1(5):119–27.
2. Vlaicu ID, Olar R, Marinescu D, Lazar V, Badea M. Physicochemical and thermal characterisation of new Co(II) complexes with pyrazole derivatives. J Therm Anal Calorim. 2013;113:1337–43.
3. Vlaicu ID, Constand M, Olar R, Marinescu D, Grecu MN, Lazar V, Chifiriuc MC, Badea M. Thermal stability of new biologic active copper (II) complexes with 5,6-dimethylbenzimidazole. J Therm Anal Calorim. 2013;113:1369–77.
4. Badea M, Vlaicu ID, Olar R, Constand M, Bleotu C, Chifiriuc MC, Măruţescu L, Lazar V, Grecu MN, Marinescu D. Thermal behaviour and characterisation of new biologically active Cu(II) complexes with benzimidazole as main ligand. J Therm Anal Calorim. 2014;118:1119–33.
5. Olar R, Vlaicu ID, Chifiriuc MC, Bleotu C, Stănică N, Vasile Scăeţeanu G, Silvestro L, Dulea C, Badea M. Synthesis, thermal analysis and biological characterisation of some new nickel (II) complexes with unsaturated carboxylates and heterocyclic N-donor ligands. J Therm Anal Calorim. 2017;127:731–41.
6. Olar R, Calu L, Badea M, Chifiriuc MC, Bleotu C, Velescu B, Stoica O, Ioniţă G, Stănică N, Silvestro L, Dulea C, Uivarosi V. Thermal behaviour of some biologically active species based on complexes with a triazolopyrimidine pharmacophore. J Therm Anal Calorim. 2017;127:685–96.
7. Calu L, Badea M, Cerc Korošec R, Bukovec P, Daniliuc C, Chifiriuc MC, Măruţescu L, Ciulică C, Şerban G, Olar R. Thermal behaviour of some novel biological active complexes with a triazolopyrimidine pharmacophore. J Therm Anal Calorim. 2017;127:697–708.
8. Narasimhan B, Sharma D, Kumar P. Biological importance of imidazole nucleus in new millenium. Med Res Chem. 2011;20:1119–40.
9. Abdul-Ghani A-S, Abu-Kijleh L, Qazzaz M. Effect of bis(acetato)tetrakis(imidazole)copper(II) in delaying the onset and reducing the mortality rate of strychnine- and thiosemicarbazide-induced convulsions. Biol Trace Elem Res. 2004;101:87–95.
10. Abdul-Ghani A-S, Abu-Hijleh A-L, Nahas N, Amin R. Hypoglycemic effect of copper (II) acetate imidazole complexes. Biol Trace Elem Res. 1996;54:143–51.
11. Bolos CA, Papazisis KT, Kortsaris AH, Voyazi S, Zambouli D, Kyriakidis DA. Antiproliferative activity of mixed-ligand dien-Cu(II) complexes with thiazole, thiazoline and imidazole derivatives. J Inorg Biochem. 2002;88:25–36.
12. Sigel H. Ternary complexes in solution. 34. Discriminating and stability increasing properties of the imidazole moiety in mixed-ligand complexes. Inorg Chem. 1980;19:1411–3.

13. Bernarducci EE, Bharadwaj PK, Lalancette RA, Korgh-Jesperson K, Potenza JA, Schugar MJ. Molecular structures, electronic spectra and ESR spectra of bis(4,4'5,5'-tetramethyl-2,2'-biimidazole)copper(II)dinitrate and bis(4,4',5,5'-tetramethyl-2,2' biimidazole)zinc(II)$_{0.90}$copper$_{0.90}$dinitrate. Inorg Chem. 1983;22:3911–20.
14. Tabrizi L, McArdle P, Ektefan M, Chiniforoshan H. Synthesis, crystal structure, spectroscopic and biological properties of mixed ligands of cadmium (II), cobalt(II) and manganese (II) valproate with 1,10-phenanthroline and imidazole. Inorg Chim Acta. 2016;439:138–44.
15. Jin S, Luo YT, Wang D, Shi J, Li SW, Shen SH, Xu YJ. Construction of five noncovalent-bonded supramolecules from reactions of cadmium (II) and zinc (II) with imidazole/benzimidazole and carboxylate ligands. Z Anorg Allg Chem. 2014;640(8–9):1717–26.
16. Wang YY, Shi Q, Shi Q-Z, Gao Y-C, Zhou Z-Y. Syntheses, characterization and crystal structure of copper (II) α, β-unsaturated carboxylate complexes with imidazole. Polyhedron. 1999;18:2009–15.
17. Hernandez J, Avila M, Jimenez-Vazquez HA, Duque J, Reguera E. Copper dimer with acetate-2-ethylimidazole as ligands. Synth React Inorg Met Org Chem. 2015;45(3):342–5.
18. Wang YY, Zhou LJ, Shi Q, Shi QZ, Gao YC, Hou X. Novel trinuclear copper (II) complexes with α, β-unsaturated carboxylates and imidazole. Trans Met Chem. 2002;27:145–8.
19. Xiong Z, Yuan P, Xie Z, Li G. Three transition-metal polymers from imidazole dicarboxylates-bearing methoxyphenyl groups: syntheses, crystal structures and properties. Supramol Chem. 2014;26(5–6):346–57.
20. Sun Y-G, Guo M-Y, Xiong G, Ding F, Wang L, Jiang B. Hydrothermal synthesis, structure and photoluminiscence of four complexes based on 1H-imidazole-4,5-dicarboxylate or 1H-imidazole-2-carboxylate ligands. J Coord Chem. 2010;63(24):4188–200.
21. Wang D-P, Chen Y-G, Wang H-Y, Zhang C-J, Tang Q. Syntheses, crystal structures and properties of four new coordination compounds of transition metals and imidazoledicarboxylic acid derivatives. J Coord Chem. 2011;64:2824–33.
22. Wang F, Chen ZN, Li ZF, Li G. Syntheses, crystal structures and thermal properties of two complexes built by imidazole-based multi-carboxylate ligands. Russ J Coord Chem. 2015;41(8):510–7.
23. Nakamoto K. Infrared and Raman Spectra of Inorganic and Coordination Compounds. New York: Wiley; 1986.
24. Morzyk-Ociepa B, Różycka-Sokołowska E, Michalska D. Revised crystal and molecular structure, FT-IR spectra and DFT studies of chlorotetrakis(imidazole)copper(II) chloride. J Mol Struct. 2012;1028:49–56.
25. Oldham C. Carboxylates, squarates and related species. In: Wilkinson G, Gillard RD, McCleverty JA, editors. Comprehensive coordination chemistry. Oxford: Pergamon Press; 1987.
26. Deacon GB, Philips RJ. Relationships between the carbon-oxygen stretching frequencies of carboxylato complexes and the type of carboxylate coordination. Coord Chem Rev. 1980;33:227–50.
27. Agulló-Rueda F, Calleja JM, Martini M, Spinolo G, Cariati F. Raman and infrared spectra of transition metal halide hexahydrates. J Raman Spectrosc. 1987;18(7):485–91.
28. Lever ABP. Inorganic electronic spectroscopy. Amsterdam: Elsevier; 1986.
29. König E. The Nephelauxetic effect. Calculation and accuracy of the interelectronic repulsion parameters I. Cubic high-spin d^2, d^3, d^7 and d^8 systems. Struct Bond. 1972;9:175–372.
30. Sacconi L, Mani F, Bencini A. Nickel. In: Wilkinson G, Gillard RD, McCleverty JA, editors. Comprehensive coordination chemistry. Oxford: Pergamon Press; 1987.
31. Mahmoud WH, Deghadi RG, Mohamed GG. Preparation, geometric structure, molecular docking thermal and spectroscopic characterization of novel Schiff base ligand and its metal chelates. J Therm Anal Calorim. 2017;127:2149–71.